Bistable spin-state switching characteristic of a charge-neutral iron(II) complex

Senthil Kumar Kuppusamy,[a*] Lea Spieker,[b] Benoît Heinrich,[c] Soma Salamon[b], Manual Gruber,[b] Heiko Wende,[b] and Mario Ruben [a,d,e]

[a]Institute of Quantum Materials and Technologies (IQMT),
Karlsruhe Institute of Technology (KIT), Hermann-von-Helmholtz-Platz 1,
76344 Eggenstein-Leopoldshafen, Germany. E-mail: senthil.kuppusamy2@kit.edu

[b]University of Duisburg-Essen,
Faculty of Physics and Center for Nanointegration Duisburg-Essen (CENIDE),
Lotharstraße 1, 47057 Duisburg, Germany.

[c]Institut de Physique et Chimie des Matériaux de Strasbourg (IPCMS),
CNRS-Université de Strasbourg, 23, rue du Loess, BP 43,
67034 Strasbourg Cedex 2, France.

[d]Institute of Nanotechnology (INT),
Karlsruhe Institute of Technology (KIT),
Hermann-von-Helmholtz-Platz 1,
76344 Eggenstein-Leopoldshafen, Germany.

[e]Centre Européen de Sciences Quantiques (CESQ)
Institut de Science et d'Ingénierie, Supramoléculaires (ISIS),
8 allée Gaspard Monge, BP 70028,
67083 Strasbourg Cedex, France.

Abstract

Spin-crossover (SCO) complexes that show abrupt and hysteretic spin-state switching characteristics—termed as bistable spin-state switching—are proposed suitable to realize molecule-based switching and memory elements. For realistic applications, spin-state switching needs to be demonstrated in the thin film state, requiring vacuum sublimation of SCO complexes to fabricate clean and impurity-free thin films. Charge-neutral iron(II) complexes are a class of SCO complexes that are reported to undergo sublimation, and their spin-state switching characteristics in the thin film state have been studied. However, hysteretic SCO in the thin film state is a scarcely observed phenomenon, requiring the development of iron(II) charge-neutral complexes that can undergo bistable spin-state switching in the bulk and thin film states. Herein, we report a new iron(II) charge-neutral complex—[Fe(H_2Bpz$_2$)$_2$4,4'-Br$_2$-bpy] (H_2Bpz$_2$ = dihydrobis(pyrazol-1-yl)borate; 4,4'-Br$_2$-bpy = 4,4'-dibromo-2,2'-bipyridine)—that undergoes abrupt and hysteretic spin-state switching in the bulk-state with $T_{1/2}$ = 113 K and $\Delta T_{1/2}$ = 13 K at a scan rate of 0.25 K/min. The HS-to-LS switching of the complex is scan-rate-dependent, whereas the LS-to-HS switching is scan-rate-independent. Moreover, a reverse-SCO phenomenon was observed upon heating the sample in the 78 K-105 K temperature range at a scan rate of 3 K/minute. However, the reverse SCO was not observed when the complex was studied at scan rates of 1 and 0.5 K/min. Such observations indicate the presence of a kinetically trapped HS-fraction (frozen-in effect) during the HS-to-LS switching, when the sample was studied at the scan rate of 3 K/min. Crucially, the complex can be sublimed; efforts are on to elucidate the nature of SCO in the thin film state. Overall, a simple and easy to prepare sublimable complex—[Fe(H_2Bpz$_2$)$_2$4,4'-Br$_2$-bpy]—shows bistable spin-state switching characteristics that can be leveraged to fabricate spin-state switchable thin film architectures.

Keywords: Molecular magnetism; Bistability; Spin-crossover; Iron(II) complexes

Introduction

Molecule-based materials that can undergo spin-state switching in response to an external perturbation—temperature, light, pressure, mechanical stretching, or electric field, for example—are proposed as active elements in molecule-based switching and memory elements. First-row transition metal complexes featuring d^4-d^7 electronic configuration, especially iron(II) complexes, that show reversible interconversion between the low- and high-spin states—termed as spin-crossover (SCO)—are a class of switchable materials that can undergo abrupt and hysteretic —bistable—spin-state switching suitable for device applications.[1–4] For practical device applications, hysteretic switching needs to be realized in the thin film state. Preparation of thin films of SCO complexes requires solution processing or vacuum sublimation.[5–10] On a comparative scale, vacuum sublimation is a cleaner process than the solution processing because molecular complexes can be directly deposited on a substrate in a high vacuum environment, avoiding the contamination of thin films with external impurities and impurities that might be present in a solvent. Charge-neutral SCO complexes are a class of SCO complexes that can undergo sublimation.[5,10] $[Fe(H_2Bpz_2)_2(L)]$, H_2Bpz_2 = dihydrobis(pyrazol-1-yl)borate; L = 2,2'-bipyridine or 1,10-phenanthroline, family of complexes are one such class of charge-neutral complexes that can be sublimed.[11] The complexes are also of interest in view of their functionalization propensity that can be leveraged to tune the spin-state switching characteristics[12–14] and assemble them in the thin film state following molecular self-assembly principles[15] or as micro-heterogeneous architectures, such as vesicles.[16]

However, to the best of our knowledge, hysteretic SCO in $[Fe(H_2Bpz_2)_2L]$ family of complexes is rarely observed even in the bulk-state.[11,17,18] A few studies reporting SCO in the thin film state with nominal hysteresis widths is restricted to thick films of $[Fe(H_2Bpz_2)_2(L)]$ on glass and Kapton-tape substrates.[19] Therefore, it is necessary to search for a molecular complex that can undergo hysteretic SCO in the bulk and thin film states. Such realization needs systematic studying of $[Fe(H_2Bpz_2)_2L]$-based complexes by varying chemical substituents at the 2,2'-bipyridine or 1,10-phenanthroline ligand skeletons. In the course of one such attempt, we have observed that a sublimable charge-neutral iron(II) complex—$[Fe(H_2Bpz_2)_2(4,4'\text{-}Br_2\text{-}bpy)]$ (H_2Bpz_2 = dihydrobis(pyrazol-1-yl)borate; L = 4,4'-dibromo-2,2'-bipyridine) (Figure 1)—undergoes temperature-induced bistable spin-state switching in the bulk-state. In the following sections, we report on the structural characterization and the bulk-state SCO characteristic of the complex.

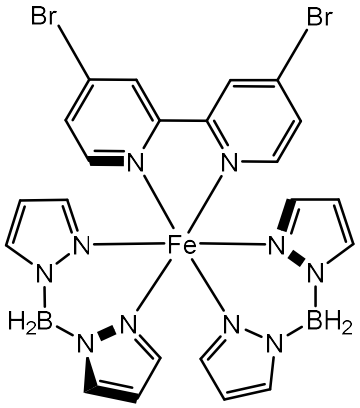

$[Fe(H_2Bpz_2)_2(4,4'\text{-}Br_2\text{-}bpy)]$

Figure 1. Molecular structure of $[Fe(H_2Bpz_2)_2(4,4'\text{-}Br_2\text{-}bpy)]$.

Results

Preparation and characterization of [Fe(H_2Bpz_2)$_2$(4,4'-Br_2-bpy)]

The complex was prepared in a straightforward manner by treating a solution of 4,4'-dibromo-2,2'-bipyridine (1), in chloroform and methanol solvent mixture, with the methanolic solution of precursor charge-neutral iron(II) complex (2),[20] as depicted in Scheme 1. The procedure yielded [Fe(H_2Bpz_2)$_2$(4,4'-Br_2-bpy)] as a pale-green powder. This complex was satisfactorily characterized with elemental analysis, see experimental section for details. Attenuated total reflectance-infrared (ATR-IR) spectroscopic studies of the complex revealed the presence of molecular vibrations corresponding to the ligand fragments. Noteworthy are the B-H stretching frequencies corresponding to dihydrobis(pyrazol-1-yl)borate ligand—2420 cm^{-1} and 2394 cm^{-1} ($\nu_{asym.}$ [-BH_2]) 2300 cm^{-1} and 2282 cm^{-1} ($\nu_{sym.}$ [-BH_2]). Three batches of the complex—a, b, and c—were prepared.

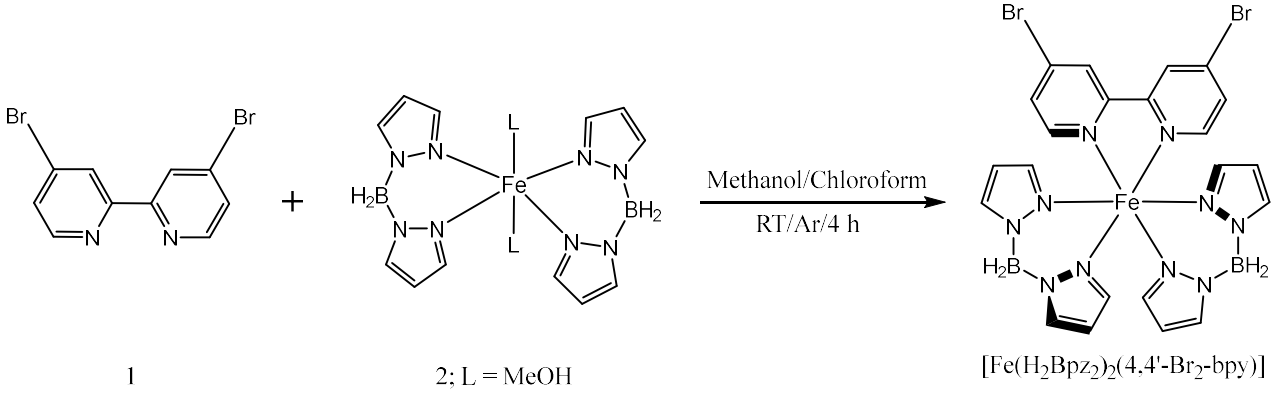

Scheme 1. Preparation of [Fe(H_2Bpz_2)$_2$(4,4'-Br_2-bpy)].

Spin-state switching characteristics of [Fe(H_2Bpz_2)$_2$(4,4'-Br_2-bpy)] in the bulk-state

For magnetic measurements, a pale-green microcrystalline form of the complex was used after a gentle grinding. The sample used in the first set of experiments is hereinafter referred to as batch a, for reasons discussed in the following paragraph. The complex—batch a—showed an abrupt and incomplete HS-to-LS switching in the cooling branch of the first cycle measured at a 3 K/min scan rate, as shown in Figure 2a. Heating the sample resulted in the decrease of χT value starting from 78 K, and a pure LS state—as inferred from the ^{57}Fe Mössbauer spectroscopic studies discussed below—is observed around 105 K. The decrease in the χT value with increasing temperature is termed as reverse-SCO and indicative of kinetic trapping of a fraction of molecules in the HS-state—known as the frozen-in effect—whose switching dynamics is slower than the scan rate. Remarkably, a complete HS-to-LS switching is observed at scan rates of 1 K/min, 0.5 K/min, and 0.25 K/min, confirming that cooling the sample at 3 K/min traps a fraction of the sample in the HS state. To further elucidate the role of fast scan rates in trapping the HS-fraction, studies were performed at 5 K/min and 10 K/min scan rates, as depicted in Figure 2b. Such studies revealed an increase in the HS-fraction with increasing scan rate, resulting in the occurrence of pronounced reverse-SCO (Figure 2b). Notably, complete reverse SCO from the HS-to-LS state was not observed at the scan rates of 5 K/min and 10 K/min. Such occurrence contrasts with the complete reverse SCO observed in the 3 K/min scan rate. Interestingly, the sample showed scan rate-dependent switching only in the HS-to-LS switching branch; the abrupt LS-to-HS switching process is scan rate independent. Overall, a scan-rate-dependent hysteretic SCO was observed for batch a of the complex—thermal hysteresis widths ($\Delta T_{1/2}$) of 18 K and 13 K were observed at the scan rates of 1 K/min and 0.25 K/min, respectively, as shown in Figure 2a.

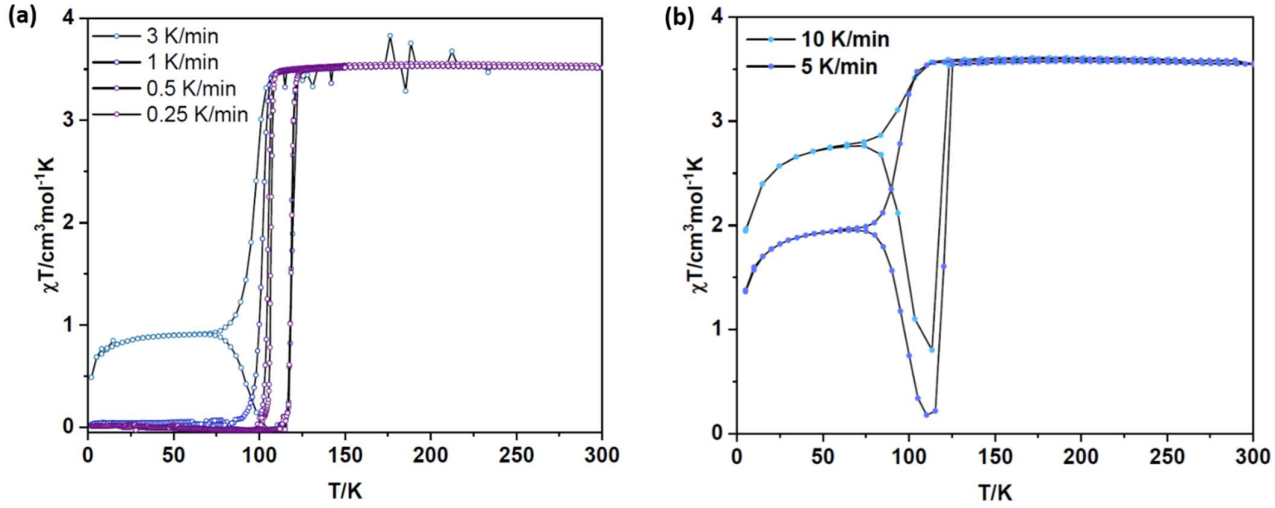

Figure 2. Scan-rate-dependent spin-state switching characteristics of $[Fe(H_2Bpz_2)_2(4,4'\text{-}Br_2\text{-}bpy)]$ (batch a). (a) χT versus T plots of batch a at 3 K/min, 1 K/min, 0.5 K/min, and 0.25 K/min scan rates. (b) χT versus T plots of batch a at 5 K/min and 10 K/min scan rates. The spikes in the data measured at 3 K/min are artefacts.

To check for reproducibility of the spin-state switching characteristics of the complex, a fresh batch of it was prepared, hereinafter referred to as batch b. The batch showed similar hysteretic SCO at a scan rate of 3 K/min as observed for batch a. However, the magnitude of reverse SCO observed for batch b is smaller than the one observed for batch a. Such difference in the magnitude of reverse SCO prompted us to prepare another fresh batch of sample, hereinafter referred to as batch c. Batch c showed comparable spin-state switching characteristics and similar magnitude of reverse SCO as observed for b.

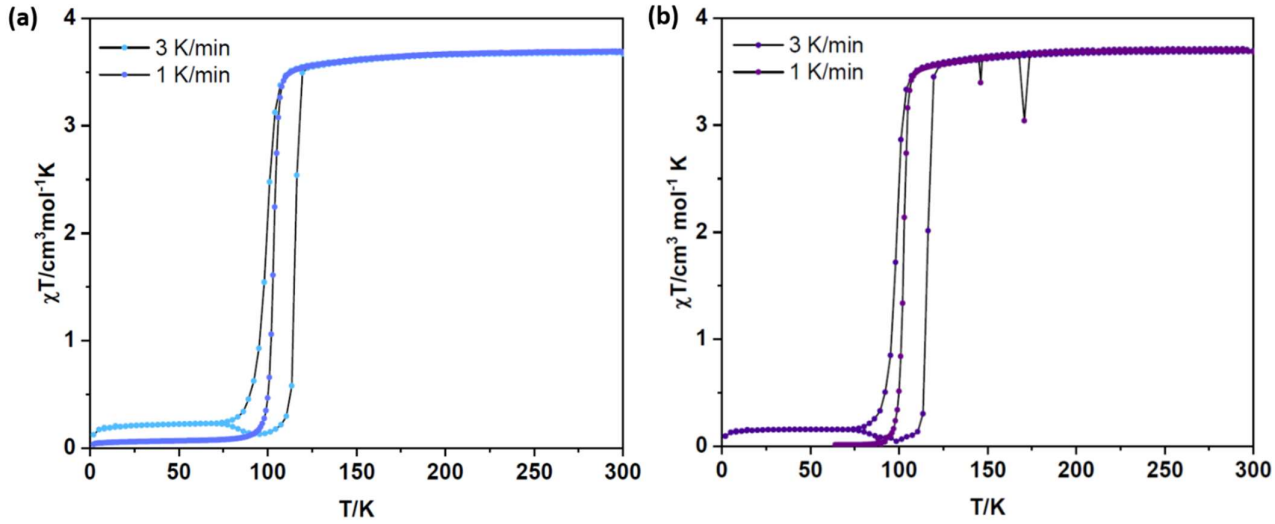

Figure 3. Spin-state switching characteristics of $[Fe(H_2Bpz_2)_2(4,4'\text{-}Br_2\text{-}bpy)]$ at varying scan-rates. (a) χT versus T plots of (a) batch b and (b) batch c at 3 K/min and 1 K/min scan rates. Only HS-to-LS switching branch is measured in the second cycle, considering the scan-rate-independent nature of the LS-to-HS switching process.

To evaluate the effect of time on the spin-state switching properties, a second set of measurements on batch c was performed after eight months of the first set of measurements depicted in Figure 3(b). The results of the second set of measurements shown in Figures 4(a) and (b) reveal the reproducible nature of the spin-state switching

properties of batch c. Moreover, measurements performed at faster scan rates of 5 K/min and 10 K/min than the ones shown in Figure 4(a) indicate the occurrence of reverse SCO. Crucially, a measurement performed at 2 K/min after the fast scans revealed a drastic decrease in the magnitude of reverse SCO and almost complete HS-to-LS state is observed. The observation indicates that the conversion between complete and incomplete HS-to-LS switching processes can be reversibly achieved by varying the scan rate. Briefly, the sample withstood the test of time at least for eight months.

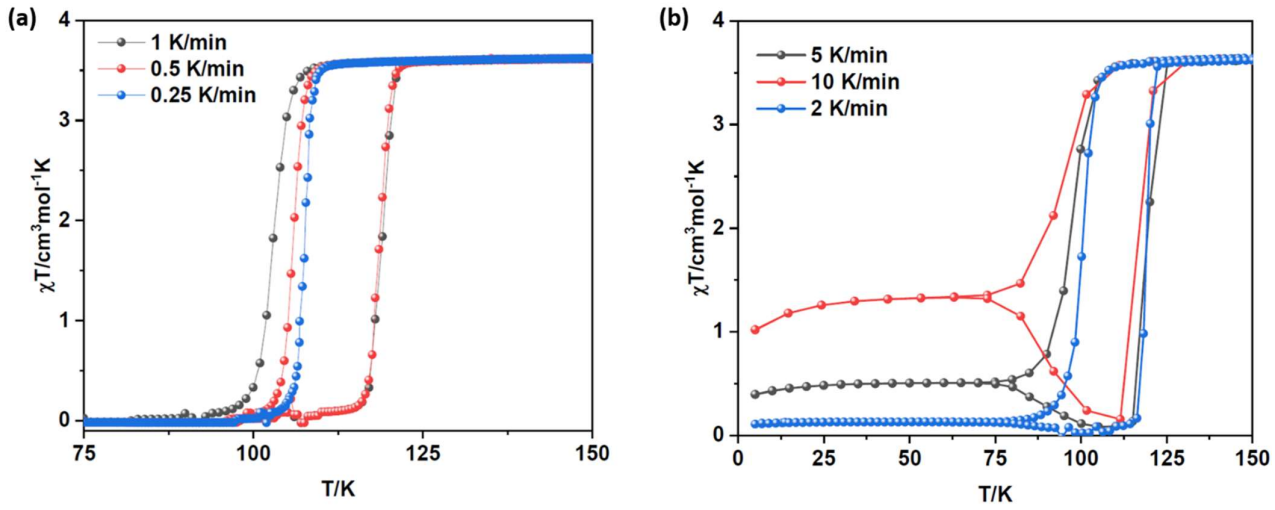

Figure 4. Spin-state switching characteristics of batch c at varying scan-rates. (a) χT versus T plots obtained from 1 K/min, 0.5 K/min, and 0.25 K/min scan rates. Only HS-to-LS switching branch is measured at the scan rate of 0.25 K/min, considering the scan-rate-independent nature of LS-to-HS switching. (b) χT versus T plots obtained from 5 K/min, 10 K/min, and 2 K/min scan rates.

The spin-state switching parameters of the batches b and c—$T_{1/2}$ = 109 K and $\Delta T_{1/2}$ = 13 K —at a scan rate of 1 K/min are comparable with the values obtained for batch a at the same scan rate, indicating that [Fe(H_2Bpz$_2$)$_2$(4,4'-Br_2-bpy)] can be prepared in a reproducible manner and the switching characteristics of the batches are comparable, except for the magnitude of reverse SCO.

To unambiguously elucidate the reverse SCO in batch a and to elucidate the purity of the spin-states, ^{57}Fe Mössbauer spectroscopic studies were performed. An abrupt cooling of batch a from 300 K to 10 K, via a 60 K measurement step, resulted in the formation of a phase composed of about 85.1% molecules in the HS state (Figure 5). Heating resulted in the increase of LS fraction, as observed at 60 K and 80 K, and a complete LS state is observed at 100 K, confirming the occurrence of reverse SCO. Further heating of the sample resulted in the increase of HS fraction, as observed at 120 K, indicating LS-to-HS switching, and a pure HS state is obtained at 160 K (Figure 6). Overall, the results obtained from the ^{57}Fe Mössbauer spectroscopic studies are in line with the χT versus T plots shown in Figure 2a—the occurrence of reverse SCO and spin-state switching resulting in the formation of pure LS and HS states are confirmed.

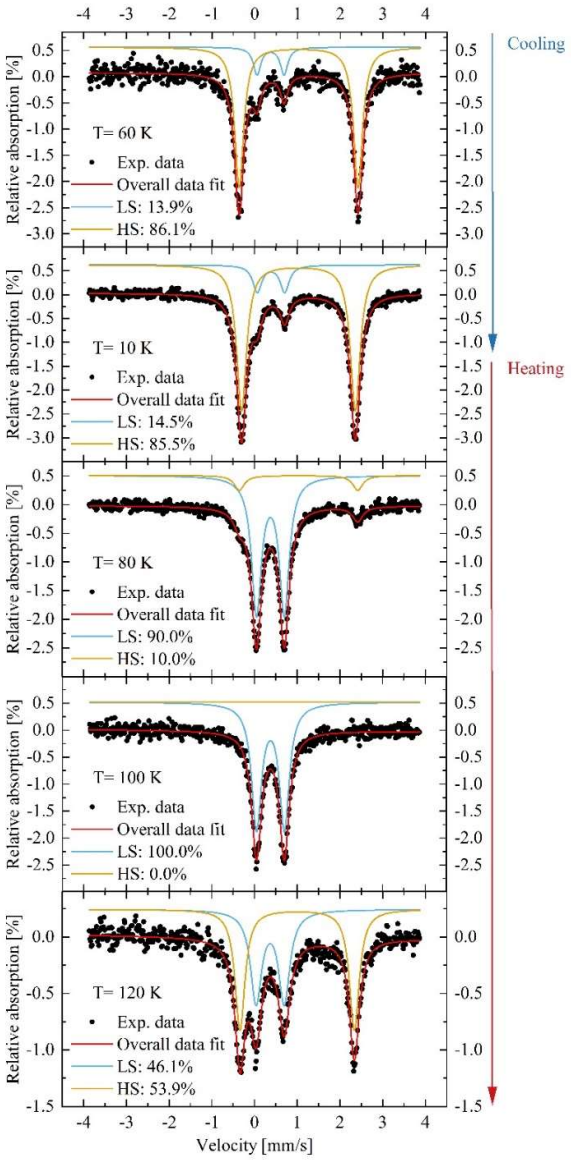

Figure 5. Variable-temperature ^{57}Fe Mössbauer spectra of batch a. The sample was abruptly cooled from 300 K to 10 K, via a 60 K measurement step, trapping the complex in a predominantly HS-state (85.5% at 10 K). Heating the sample induced reverse HS-to-LS switching around 80 K, and a pure LS-state is observed at 100 K, elucidating the occurrence of reverse SCO.

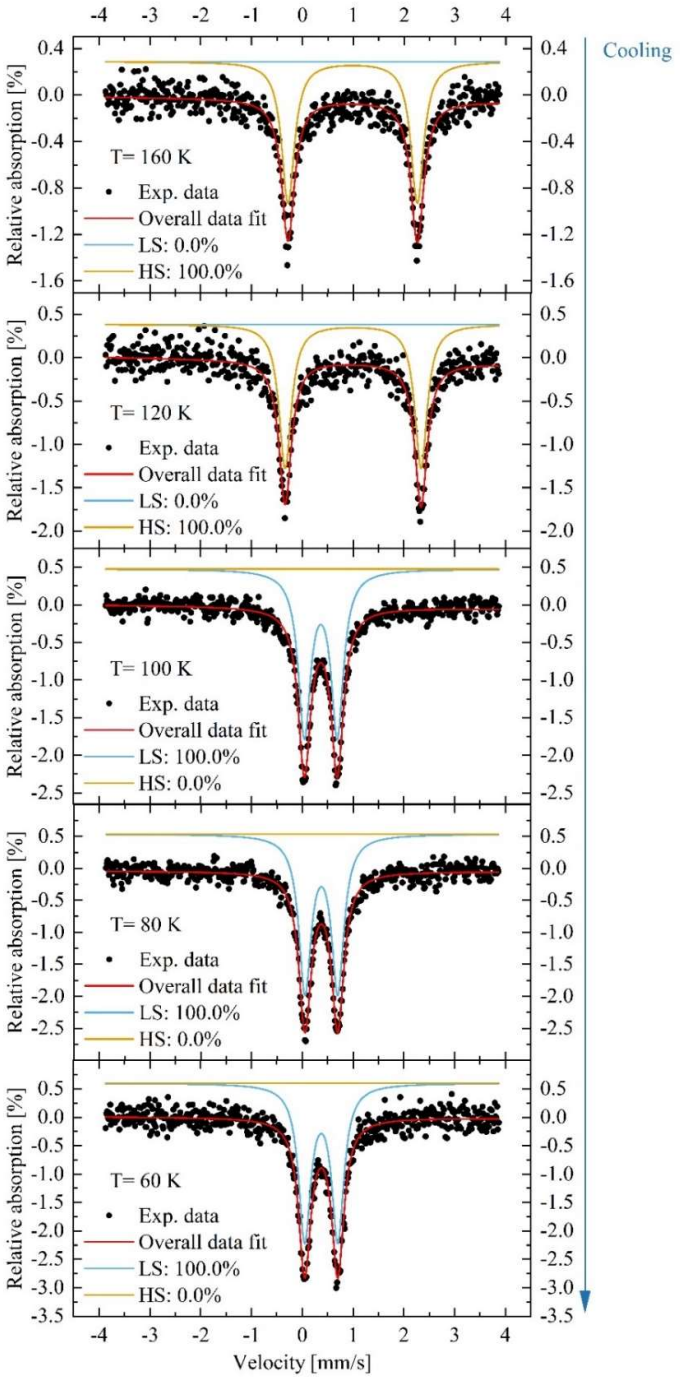

Figure 6. Variable-temperature ^{57}Fe Mössbauer spectra of batch a. The sample was slowly cooled from 160 K to 60 K, revealing the onset of complete HS-to-LS switching around 100 K, in line with the χT versus T plots shown in Figure 2a.

Infrared spectroscopic, small- and wide-angle X-ray scattering, and thermogravimetric studies of batches a and b

To shed light on the differing reverse SCO characteristics associated with batches a and b, attenuated total reflectance-infrared (ATR-IR) spectroscopic, small- and wide-angle X-ray scattering (SWAXS), and thermogravimetric (TG) studies were performed. The studies are not performed for batch c, considering the comparable nature of its spin-state switching characteristic with b. The ATR-IR spectra of a and b are identical (Figure 7), elucidating that molecular vibrations giving rise to the spectroscopic signatures are the same in the batches. This indicates that there are minute differences in the packing of molecules in the crystal lattice which evades IR spectroscopic detection.

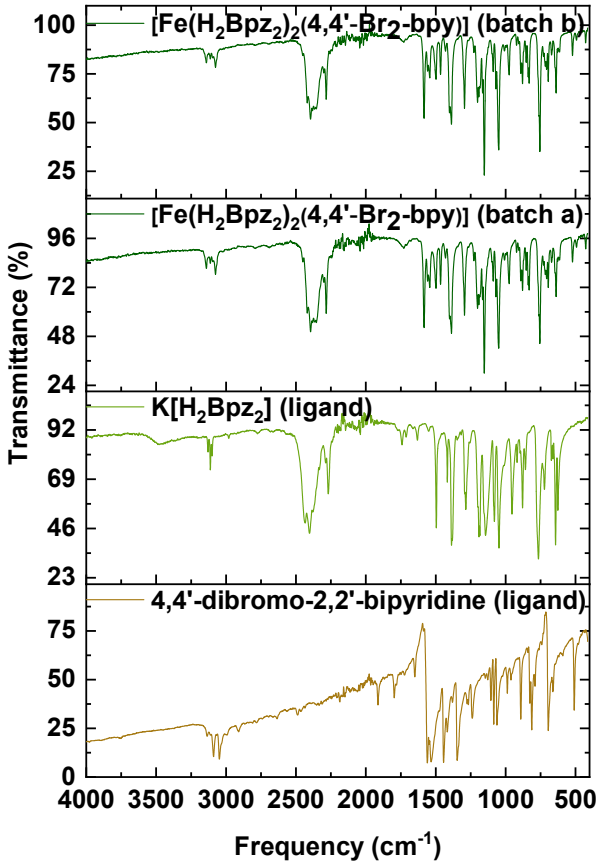

Figure 7. ATR-IR spectra of ligands and complexes measured at RT. The spectra of batches a and b can be considered as a superposition of vibrations of 4,4'-dibromo-2,2'-bipyridine and dihydrobis(pyrazol-1-yl)borate ligands. The comparable nature of the IR spectra of the batches reveals that molecular structure of the complex in the batches is the same.

To get insights into the nature of the molecular organization in the lattices of batch a and c, SWAXS studies were performed. The studies revealed the well-defined crystalline nature of samples a and b (Figure 8a). Moreover, both the samples feature the same crystalline structure as inferred from the patterns depicted in Figure 8a, indicating no discernible variations in the molecular organization in the lattices of a and b. Another factor that could contribute to the differing SCO profiles is the presence or absence of lattice solvent. To shed light on this aspect, thermogravimetric analyses (TGA) of the samples were performed as shown in Figure 8b. The analyses revealed the

absence of lattice solvent in the lattices of batches a and b. The weight loss starting from 410 K in the traces shown in Figure 8b is due to the degradation of the complex. The results obtained from TGA analyses are in agreement with the elemental analyses data (see experimental section) of the batches a and b, showing the absence of lattice solvents. Moreover, the comparable nature of elemental analyses data obtained for a and b and the match with the expected molecular formula also rule out other possible contaminations—for example, ligand fragments or co-crystallized precursor complex—in the samples.

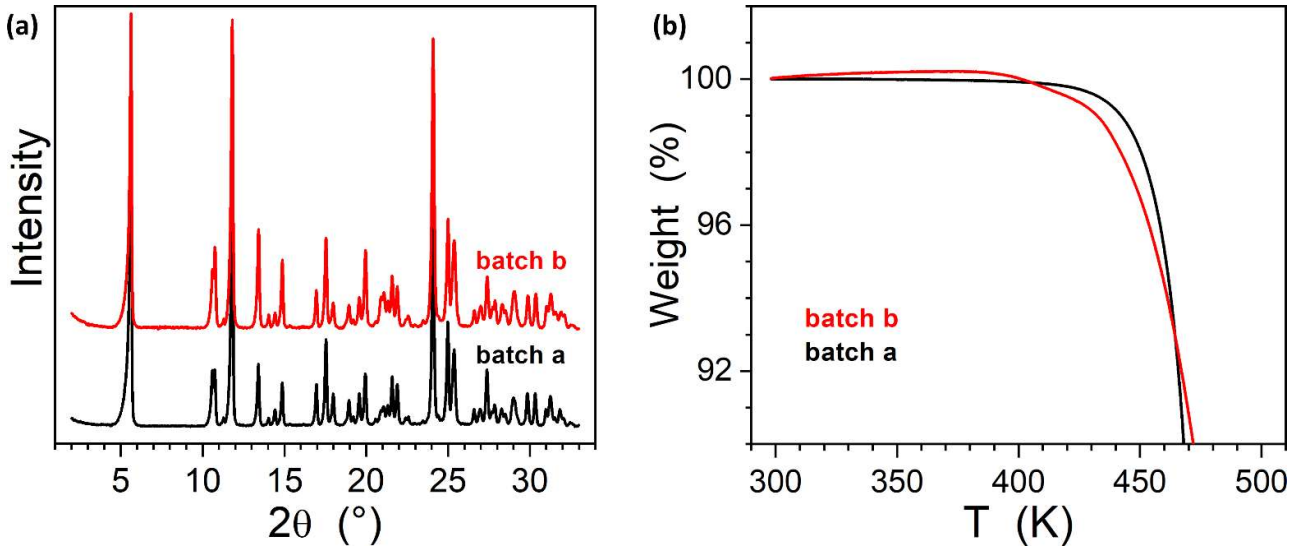

Figure 8. Small- and wide-angle X-ray scattering studies and thermogravimetric analyses of batches a and b. The comparable nature of (a) SWAXS patterns of a and b indicates that molecular organization in their lattice is the same. (b) TGA profiles showing similar thermal characteristics indicate the absence of lattice solvent molecules in the samples.

Discussion

Complex [Fe(H_2Bpz$_2$)$_2$(4,4'-Br$_2$-bpy)] showed one of the largest thermal hysteresis values ($\Delta T_{1/2}$ = 13 K; SR = 0.25 K/min) reported for [Fe(H_2Bpz$_2$)$_2$(L)] family of complexes.[17,18] The two complexes that are known to show meaningful thermal hysteresis loops are [Fe(H_2Bpz$_2$)$_2$(L1)], L1 = TTF-fused dipyrido-[3,2-a:2',3'-c]phenazine, and [Fe(H_2Bpz$_2$)$_2$(L2)], L2 = 2,2'-bipyridine-5,5'-dicarboxylate, reported by Pointillart et al.[17] and Guo et al.,[18] respectively. The first and second complexes show thermal hysteresis widths of 48 K ($T_{1/2}$ = 143 K) and 10 K ($T_{1/2}$ = 128 K), respectively. In the studies by Pointillart et al. and Guo et al., the scan rates used in the measurements were not reported, and attempts were not made to study the scan-rate-dependent evolution of $\Delta T_{1/2}$. Another notable aspect of the SCO observed for [Fe(H_2Bpz$_2$)$_2$(4,4'-Br$_2$-bpy)] is the formation of mixed-spin (HS and LS) proportion in the HS-to-LS switching branch at scan rates around 3 K and above. The kinetically trapped residual HS-states underwent HS-to-LS switching with temperature increase, indicating the thermal-energy-mediated crossing of the kinetic energy barrier. Though the process known as reverse spin-crossover is observed for spin-crossover systems,[4,21–24] it has not been observed for [Fe(H_2Bpz$_2$)$_2$(L)] systems previously, to the best of our knowledge. An unsolved aspect of the reverse SCO observed for [Fe(H_2Bpz$_2$)$_2$(4,4'-Br2-bpy)] is the differing magnitude of the phenomenon in batches a and batches b and c, despite batches a and b showing comparable features obtained from ATR-IR spectroscopic, SWAXS, and thermogravimetric analyses. A similar observation was made in the case of a binuclear iron(II) complex, whose polymorphs showed markedly different spin-state switching characteristics, despite featuring comparable spectral characteristics.[25] Our recent report dealing with a mononuclear iron(II) complex showing markedly different SCO characteristics despite showing comparable SWAXS patterns is another example.[26]

Establishment of a relation between molecular structure and SCO property—for example, what contributes to reverse SCO in [Fe(H_2Bpz_2)$_2$(4,4'-Br2-bpy)]? —in the bulk-state requires single-crystal X-ray structure determination of a molecule under investigation in the LS and HS states. Despite the best of our efforts, we were unable to obtain single-crystals of [Fe(H_2Bpz_2)$_2$(4,4'-Br_2-bpy)]. This prevented us from experimentally elucidating variation of angular parameters and intermolecular interactions accompanying the spin-state switching process. However, we speculate contributing roles of Br-H and Br-π intermolecular interactions, among other unknown intermolecular interactions, in inducing abrupt and hysteretic SCO because such interactions are known to organize and mediate elastic interactions between molecules in crystal lattices.[27]

The hysteretic nature of the spin-state switching observed for [Fe(H_2Bpz_2)$_2$(4,4'-Br_2-bpy)] in the bulk-state is encouraging to study the switching characteristic of the complex in the thin film state by subliming it onto suitable substrates. Such studies are important to progress toward SCO-based applications and understand molecule-substrate interactions governing spin-state switching characteristics of surface-bound films. The observation of hysteretic spin-state switching in surface-bound films of sublimable SCO complexes is scarcely reported.[28,29] Hysteretic switching characteristic of thin- and thick-films of complex [Fe^{II}((3,5-$(CH_3)_2Pz)_3BH)_2$] bound on Cu(111),[30] quartz,[28] and SiO_2[29] has been demonstrated. However, the reported hysteresis profiles are asymmetric in nature. Moreover, the spin-state switching observed for the complex in the bulk and thin film states is gradual. For practical applications, surface-bound films that show abrupt, hysteretic, and complete SCO with square-like or symmetric switching profiles are desirable; such elucidation is unprecedented, to the best of our knowledge. The structurally compact nature of [Fe(H_2Bpz_2)$_2$(4,4'-Br_2-bpy)] and $\Delta T_{1/2}$ = 13 K observed in the bulk-state presents us with an opportunity to search for the elusive bistable switching profile in the thin film state.

Perspective

Spin-state switching in molecular complexes is extremely sensitive to structural variations. Such property requires the establishment of a structure-SCO property relationship by systematically varying substituents in a ligand framework. One complementary and less explored pathway is the preparation of isomeric SCO complexes,[31,32] featuring the same molecular formula and different functional group placement. In this context, we have extended the present study by preparing a new complex—[Fe(H_2Bpz_2)$_2$(5,5'-Br_2-bpy)], where 5,5'-Br_2-bpy is 5,5'-dibromo-2,2'-bipyridine (Figure 9)—and the complex is an isomer of [Fe(H_2Bpz_2)$_2$(4,4'-Br_2-bpy)]. Variable temperature magnetic measurements revealed an incomplete spin-state switching characteristic of [Fe(H_2Bpz_2)$_2$(5,5'-Br_2-bpy)] in the bulk-state, as against the bistable SCO characteristics observed for [Fe(H_2Bpz_2)$_2$(4,4'-Br_2-bpy)]. Such observations elucidate a pathway to control spin-state switching characteristics in iron(II) complexes.

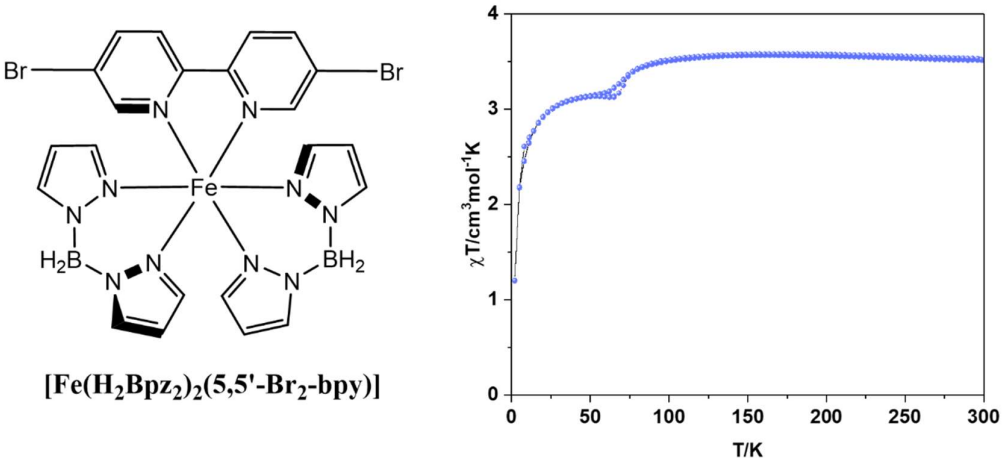

Figure 9. Molecular structure of (left) [Fe(H_2Bpz_2)$_2$(5,5'-Br_2-bpy)] and (right) its spin-state switching characteristics.

The observation of incomplete SCO in [Fe(H_2Bpz$_2$)$_2$(5,5'-Br$_2$-bpy)] at first sight is discouraging. However, the switching propensity of the complex might change in thin film state. Such a hypothesis is based on a literature report showing the SCO-active nature of a surface-bound films of complexes [Fe(H_2Bpz$_2$)$_2$(L3)], L3 = 4,7-dichloro-1,10-phenanthroline and [Fe(H_2Bpz$_2$)$_2$(L4)], L4 = 4,7-dimethyl-1,10-phenanthroline; the complexes remained trapped in the HS-state in the bulk.[12]

Summary and conclusions

A novel and easy to prepare iron(II) complex showed bistable spin-state switching characteristics in the bulk-state. The spin-state switching characteristics of the complex is reproducible, except for a variation in the magnitude of the reverse SCO between batch a and batches b and c, as demonstrated by preparing three different batches of the complex. The complex can be sublimed; enabling the study of the spin-state switching characteristic of the complex at varying coverages on a range of substrates; for example, Au(111), highly oriented pyrolytic graphite (HOPG), and indium tin oxide (ITO). In a nutshell, the occurrence of bistable SCO, in the bulk-state, and sublimation propensity of [Fe(H_2Bpz$_2$)$_2$(4,4'-Br$_2$-bpy)] is encouraging to study the complex in the thin film state, searching for magnetic bistability.

Experimental section

Materials

All the solvents used to prepare the complexes are dried by storing them on freshly activated 3 Å molecular sieves for three days. The potassium dihydro(bispyrazolyl)borate was prepared according to the literature report. 5,5'-dibromo-2,2'-bipyridine and 4,4'-dibromo-2,2'-bipyridine ligands were purchased from commercial sources and used as received.

Preparation and characterization of the complexes

Preparation of [Fe(H_2Bpz$_2$)$_2$(4,4'-Br$_2$-bpy)]: To a solution of iron (II) perchlorate hydrate (0.037 g, 0.1 mmol) in 5 ml of methanol, anionic ligand, potassium dihydro(bispyrazolyl)borate, (0.0375 g, 0.2 mmol) was added, and the mixture was stirred for 15 min and filtered to remove the precipitated $KClO_4$. This step yields a pale-yellow solution of charge-neutral precursor complex (2) shown in scheme 1. A solution of 4,4'-dibromo-2,2'-bipyridine (1) (0.032 g, 0.1 mmol) in chloroform (0.8 ml) and methanol (0.2 ml) solvent mixture was added to the filtrate, and the reaction mixture was stirred for four hours under argon protection. The reaction mixture was filtered, and the obtained precipitate was washed with methanol several times, yielding the complex as a pale-green powder. The complex was dried under vacuum overnight prior to the analyses described in the text.

Elemental analysis: Calculated for $C_{22}H_{22}B_2Br_2FeN_{10}$; C 39.81, H 3.34, N 21.10. Found for batch a: C 39.26, H 3.28, N 20.84. Found for batch b: C 39.15, H 3.28, N 21.

Preparation of [Fe(H_2Bpz$_2$)$_2$(5,5'-Br$_2$-bpy)]: The complex was prepared following the procedure used to prepare [Fe(H_2Bpz$_2$)$_2$(4,4'-Br$_2$-bpy)].

Elemental analysis: Calculated for $C_{22}H_{22}B_2Br_2FeN_{10}$; C 39.81, H 3.34, N 21.10. Found: C 38.32, H 3.09, N 20.41.

Methods

Magnetic measurements of the complexes were performed on a MPMS-3 SQUID-VSM magnetometer (Quantum Design). The temperature-dependent magnetization was recorded at an applied DC field of 0.1 T. Temperature sweeping rates of 3 K min^{-1}, 1 K min^{-1}, 0.5 K min^{-1}, and 0.25 K min^{-1} were employed. Gelatine capsules were used as sample holders in the 5 K to 300 K temperature range.

^{57}Fe Mössbauer spectra were recorded on unenriched powder samples in transmission geometry, utilizing a ~50 mCi ^{57}Co radiation source mounted on a constant-acceleration Mössbauer driving unit (WissEl GmbH). Temperature control was achieved by means of a closed-cycle cryostat (Lakeshore) using a heated sample holder assembly.

Attenuated Total Reflectance Infrared (ATR-IR) spectroscopic studies of the ligands and complexes were performed using Thermo scientific Nicolet iS50 FT-IR spectrometer.

Small- and wide-angle X-ray scattering (SWAXS) patterns of the batches a and b were obtained with a linear monochromatic Cu $K_{\alpha 1}$ beam (λ = 1.5405 Å). The beam was obtained using a sealed-tube generator equipped with a bent quartz monochromator. The samples were filled in sealed cells of adjustable path. The sample temperature was controlled within ±0.1 °C, and exposure times were of 24 h. The patterns were recorded on image plates scanned by Amersham Typhoon IP with 25 µm resolution (periodicities up to 120 Å). I(2θ) profiles were obtained from images, by using a home-developed software.

Thermogravimetric analyses of batches a and b were performed TGA measurements were performed with a TA Instruments Q50 instrument operated at a scanning rate of 5 K/ min.

Elemental analyses of the complexes were performed using Elementar vario MICRO cube elemental analyser.

Acknowledgements

The authors thank Ulrich von Hörsten for his expert technical assistance with the Mössbauer measurements. Grant agency innovation FRC is acknowledged for the financial support for the project Self-assembly of spin-crossover (SCO) complexes on graphene. M.R. thanks the DFG priority program 1928 “COORNETS” for generous support. S.S. L.S., and H.W. acknowledge the funding by the Deutsche Forschungsgemeinschaft (DFG, German Research Foundation) – Project-ID 278162697 – CRC 1242, Project A05. S.S. acknowledges financial support from CRC/TRR 247 project #388390466, sub-project B2.

References

(1) Seredyuk, M.; Znovjyak, K.; Valverde-Muñoz, F. J.; da Silva, I.; Muñoz, M. C.; Moroz, Y. S.; Real, J. A. 105 K Wide Room Temperature Spin Transition Memory Due to a Supramolecular Latch Mechanism. *J. Am. Chem. Soc.* **2022**, jacs.2c05417. https://doi.org/10.1021/jacs.2c05417.

(2) Suryadevara, N.; Mizuno, A.; Spieker, L.; Salamon, S.; Sleziona, S.; Maas, A.; Pollmann, E.; Heinrich, B.; Schleberger, M.; Wende, H.; Kuppusamy, S. K.; Ruben, M. Structural Insights into Hysteretic Spin-Crossover in a Set of Iron(II)-2,6-bis(1 *H* -Pyrazol-1-yl)Pyridine) Complexes. *Chem. – Eur. J.* **2022**, *28* (6). https://doi.org/10.1002/chem.202103853.

(3) Senthil Kumar, K.; Heinrich, B.; Vela, S.; Moreno-Pineda, E.; Bailly, C.; Ruben, M. Bi-Stable Spin-Crossover Characteristics of a Highly Distorted [Fe(1-BPP-$COOC_2H_5)_2$]$(ClO_4)_2$·CH_3CN Complex. *Dalton Trans.* **2019**, *48* (12), 3825–3830. https://doi.org/10.1039/C8DT04928A.

(4) Kulmaczewski, R.; Kershaw Cook, L. J.; Pask, C. M.; Cespedes, O.; Halcrow, M. A. Iron(II) Complexes of 4-(Alkyldisulfanyl)-2,6-Di(Pyrazolyl)Pyridine Derivatives. Correlation of Spin-Crossover Cooperativity with Molecular Structure Following Single-Crystal-to-Single-Crystal Desolvation. *Cryst. Growth Des.* **2022**, *22* (3), 1960–1971. https://doi.org/10.1021/acs.cgd.2c00005.

(5) Kumar, K. S.; Ruben, M. Sublimable Spin-Crossover Complexes: From Spin-State Switching to Molecular Devices. *Angew. Chem. Int. Ed.* **2021**, *60* (14), 7502–7521. https://doi.org/10.1002/anie.201911256.

(6) Kipgen, L.; Bernien, M.; Tuczek, F.; Kuch, W. Spin-Crossover Molecules on Surfaces: From Isolated Molecules to Ultrathin Films. *Adv. Mater.* **2021**, *33* (24), 2008141. https://doi.org/10.1002/adma.202008141.

(7) Gruber, M.; Berndt, R. Spin-Crossover Complexes in Direct Contact with Surfaces. *Magnetochemistry* **2020**, *6* (3), 35. https://doi.org/10.3390/magnetochemistry6030035.

(8) Johannsen, S.; Ossinger, S.; Grunwald, J.; Herman, A.; Wende, H.; Tuczek, F.; Gruber, M.; Berndt, R. Spin Crossover in a Cobalt Complex on Ag(111). *Angew. Chem. Int. Ed.* **2022**, *61* (12). https://doi.org/10.1002/anie.202115892.

(9) Thakur, S.; Golias, E.; Kumberg, I.; Senthil Kumar, K.; Hosseinifar, R.; Torres-Rodríguez, J.; Kipgen, L.; Lotze, C.; Arruda, L. M.; Luo, C.; Radu, F.; Ruben, M.; Kuch, W. Thermal- and Light-Induced Spin-Crossover Characteristics of a Functional Iron(II) Complex at Submonolayer Coverage on HOPG. *J. Phys. Chem. C* **2021**, *125* (25), 13925–13932. https://doi.org/10.1021/acs.jpcc.1c02774.

(10) Gakiya-Teruya, M.; Jiang, X.; Le, D.; Üngör, Ö.; Durrani, A. J.; Koptur-Palenchar, J. J.; Jiang, J.; Jiang, T.; Meisel, M. W.; Cheng, H.-P.; Zhang, X.-G.; Zhang, X.-X.; Rahman, T. S.; Hebard, A. F.; Shatruk, M. Asymmetric Design of Spin-Crossover Complexes to Increase the Volatility for Surface Deposition. *J. Am. Chem. Soc.* **2021**, *143* (36), 14563–14572. https://doi.org/10.1021/jacs.1c04598.

(11) Real, J. A.; Muñoz, M. C.; Faus, J.; Solans, X. Spin Crossover in Novel Dihydrobis(1-Pyrazolyl)Borate [$H_2B(Pz)_2$]-Containing Iron(II) Complexes. Synthesis, X-Ray Structure, and Magnetic Properties of [FeL{$H_2B(Pz)_2$}$_2$] (L = 1,10-Phenanthroline and 2,2'-Bipyridine). *Inorg. Chem.* **1997**, *36* (14), 3008–3013. https://doi.org/10.1021/ic960965c.

(12) Naggert, H.; Rudnik, J.; Kipgen, L.; Bernien, M.; Nickel, F.; Arruda, L. M.; Kuch, W.; Näther, C.; Tuczek, F. Vacuum-Evaporable Spin-Crossover Complexes: Physicochemical Properties in the Crystalline Bulk and in Thin Films Deposited from the Gas Phase. *J. Mater. Chem. C* **2015**, *3* (30), 7870–7877. https://doi.org/10.1039/C5TC00930H.

(13) Nihei, M.; Suzuki, Y.; Kimura, N.; Kera, Y.; Oshio, H. Bidirectional Photomagnetic Conversions in a Spin-Crossover Complex with a Diarylethene Moiety. *Chem. - Eur. J.* **2013**, *19* (22), 6946–6949. https://doi.org/10.1002/chem.201300767.

(14) Milek, M.; Heinemann, F. W.; Khusniyarov, M. M. Spin Crossover Meets Diarylethenes: Efficient Photoswitching of Magnetic Properties in Solution at Room Temperature. *Inorg. Chem.* **2013**, *52* (19), 11585–11592. https://doi.org/10.1021/ic401960x.

(15) Kumar, K. S.; Studniarek, M.; Heinrich, B.; Arabski, J.; Schmerber, G.; Bowen, M.; Boukari, S.; Beaurepaire, E.; Dreiser, J.; Ruben, M. Engineering On-Surface Spin Crossover: Spin-State Switching in a Self-Assembled Film of Vacuum-Sublimable Functional Molecule. *Adv. Mater.* **2018**, *30* (11), 1705416. https://doi.org/10.1002/adma.201705416.

(16) Luo, Y.-H.; Liu, Q.-L.; Yang, L.-J.; Sun, Y.; Wang, J.-W.; You, C.-Q.; Sun, B.-W. Magnetic Observation of above Room-Temperature Spin Transition in Vesicular Nano-Spheres. *J. Mater. Chem. C* **2016**, *4* (34), 8061–8069. https://doi.org/10.1039/C6TC02796B.

(17) Pointillart, F.; Liu, X.; Kepenekian, M.; Le Guennic, B.; Golhen, S.; Dorcet, V.; Roisnel, T.; Cador, O.; You, Z.; Hauser, J.; Decurtins, S.; Ouahab, L.; Liu, S.-X. Thermal and Near-Infrared Light Induced Spin Crossover in a Mononuclear Iron(II) Complex with a Tetrathiafulvalene-Fused Dipyridophenazine Ligand. *Dalton Trans.* **2016**, *45* (28), 11267–11271. https://doi.org/10.1039/C6DT00920D.

(18) Guo, Y.; Rotaru, A.; Müller-Bunz, H.; Morgan, G. G.; Zhang, S.; Xue, S.; Garcia, Y. Auxiliary Alkyl Chain Modulated Spin Crossover Behaviour of [Fe(H_2Bpz_2)$_2$(C_n-Bipy)] Complexes. *Dalton Trans.* **2021**, *50* (37), 12835–12842. https://doi.org/10.1039/D1DT01787J.

(19) Palamarciuc, T.; Oberg, J. C.; El Hallak, F.; Hirjibehedin, C. F.; Serri, M.; Heutz, S.; Létard, J.-F.; Rosa, P. Spin Crossover Materials Evaporated under Clean High Vacuum and Ultra-High Vacuum Conditions: From Thin Films to Single Molecules. *J. Mater. Chem.* **2012**, *22* (19), 9690. https://doi.org/10.1039/c2jm15094h.

(20) Ossinger, S.; Näther, C.; Tuczek, F. Bis[Dihydrobis(Pyrazol-1-yl-κN^2)Borato]Bis(Methanol-κO)Iron(II). *IUCrData* **2016**, *1* (8), x161252. https://doi.org/10.1107/S2414314616012529.

(21) Manoharan, P. T.; Sambandam, B.; Amsarani, R.; Varghese, B.; Gopinath, C. S.; Nomura, K. Ligand Dynamics Controlled Reverse Spin Cross over in Bis Pyrazolyl Pyridine Based Fe(II) Complex Cation with Metallodithiolato Anions with an Example of a Ferromagnetic 2:1 Cocrystal of Mixed Ni(III)/Ni(II) Oxidation States. *Inorganica Chim. Acta* **2011**, *374* (1), 586–600. https://doi.org/10.1016/j.ica.2011.02.081.

(22) Manikandan, P.; Padmakumar, K.; Thomas, K. R. J.; Varghese, B.; H. Onodera, and Manoharan, P. T. Lattice-Dictated Conformers in Bis(Pyrazolyl)Pyridine-Based Iron(II) Complexes: Mössbauer, NMR, and Magnetic Studies. *Inorg. Chem.* **2001**, *40* (27), 6930–6939. https://doi.org/10.1021/ic010655g.

(23) Kanetomo, T.; Ni, Z.; Enomoto, M. Hydrogen-Bonded Cobalt(II)-Organic Framework: Normal and Reverse Spin-Crossover Behaviours. *Dalton Trans.* **2022**, *51* (13), 5034–5040. https://doi.org/10.1039/D2DT00453D.

(24) Agustí, G.; Bartual, C.; Martínez, V.; Muñoz-Lara, F. J.; Gaspar, A. B.; Muñoz, M. C.; Real, J. A. Polymorphism and "Reverse" Spin Transition in the Spin Crossover System $[Co(4\text{-Terpyridone})_2](CF_3SO_3)_2 \cdot 1H_2O$. *New J. Chem.* **2009**, *33* (6), 1262. https://doi.org/10.1039/b905674b.

(25) Schneider, C. J.; Cashion, J. D.; Chilton, N. F.; Etrillard, C.; Fuentealba, M.; Howard, J. A. K.; Létard, J.; Milsmann, C.; Moubaraki, B.; Sparkes, H. A.; Batten, S. R.; Murray, K. S. Spin Crossover in a 3,5-Bis(2-pyridyl)-1,2,4-triazolate-Bridged Dinuclear Iron(II) Complex $[\{Fe(NCBH_3)(Py)\}_2(M\text{-}L^1)_2]$ – Powder versus Single Crystal Study. *Eur. J. Inorg. Chem.* **2013**, *2013* (5–6), 850–864. https://doi.org/10.1002/ejic.201201075.

(26) Kuppusamy, S. K.; Mizuno, A.; García-Fuente, A.; van der Poel, S.; Heinrich, B.; Ferrer, J.; van der Zant, H. S. J.; Ruben, M. Spin-Crossover in Supramolecular Iron(II)–2,6-Bis(1 *H* -Pyrazol-1-Yl)Pyridine Complexes: Toward Spin-State Switchable Single-Molecule Junctions. *ACS Omega* **2022**, *7* (16), 13654–13666. https://doi.org/10.1021/acsomega.1c07217.

(27) Douib, H.; Cornet, L.; Gonzalez, J. F.; Trzop, E.; Dorcet, V.; Gouasmia, A.; Ouahab, L.; Cador, O.; Pointillart, F. Spin-Crossover and Field-Induced Single-Molecule Magnet Behaviour in Metal(II)-Dipyrazolylpyridine Complexes. *Eur. J. Inorg. Chem.* **2018**, *2018* (40), 4452–4457. https://doi.org/10.1002/ejic.201800819.

(28) Iasco, O.; Boillot, M.-L.; Bellec, A.; Guillot, R.; Rivière, E.; Mazerat, S.; Nowak, S.; Morineau, D.; Brosseau, A.; Miserque, F.; Repain, V.; Mallah, T. The Disentangling of Hysteretic Spin Transition, Polymorphism and Metastability in Bistable Thin Films Formed by Sublimation of Bis(Scorpionate) Fe(II) Molecules. *J. Mater. Chem. C* **2017**, *5* (42), 11067–11075. https://doi.org/10.1039/C7TC03276E.

(29) Davesne, V.; Gruber, M.; Studniarek, M.; Doh, W. H.; Zafeiratos, S.; Joly, L.; Sirotti, F.; Silly, M. G.; Gaspar, A. B.; Real, J. A.; Schmerber, G.; Bowen, M.; Weber, W.; Boukari, S.; Da Costa, V.; Arabski, J.; Wulfhekel, W.; Beaurepaire, E. Hysteresis and Change of Transition Temperature in Thin Films of $Fe\{[Me_2Pyrz]_3BH\}_2$, a New Sublimable Spin-Crossover Molecule. *J. Chem. Phys.* **2015**, *142* (19), 194702. https://doi.org/10.1063/1.4921309.

(30) Kelai, M.; Repain, V.; Tauzin, A.; Li, W.; Girard, Y.; Lagoute, J.; Rousset, S.; Otero, E.; Sainctavit, P.; Arrio, M.-A.; Boillot, M.-L.; Mallah, T.; Enachescu, C.; Bellec, A. Thermal Bistability of an Ultrathin Film of Iron(II) Spin-Crossover Molecules Directly Adsorbed on a Metal Surface. *J. Phys. Chem. Lett.* **2021**, *12* (26), 6152–6158. https://doi.org/10.1021/acs.jpclett.1c01366.

(31) Bushuev, M. B.; Krivopalov, V. P.; Nikolaenkova, E. B.; Vinogradova, K. A.; Gatilov, Y. V. Hysteretic Spin Crossover in Isomeric Iron(II) Complexes. *Dalton Trans.* **2018**, *47* (29), 9585–9591. https://doi.org/10.1039/C8DT02223B.

(32) Kumar, K. S.; Šalitroš, I.; Moreno-Pineda, E.; Ruben, M. Spacer Type Mediated Tunable Spin Crossover (SCO) Characteristics of Pyrene Decorated 2,6-Bis(Pyrazol-1-Yl)Pyridine (Bpp) Based Fe(II) Molecular Spintronic Modules. *Dalton Trans.* **2017**, *46* (30), 9765–9768. https://doi.org/10.1039/C7DT02219K.